Ćuk-Buck Converter for Standalone Photovoltaic System

Ahmad H. El Khateb, Nasrudin Abd Rahim, and Jeyraj Selvaraj

Abstract—**This paper presents MPPT converter for battery charger. The converter combines both ćuk and buck converters to extract the maximum power from the sun while supplying a controlled constant current/voltage to the battery. The topology uses two control signals instead of one control signal; one for tracking the maximum power point, another for charging the battery providing constant current/voltage to the battery. The advantage of this converter is to exploit the maximum power of the PV array avoiding battery damage caused by variable MPPT voltage. The effectiveness of the proposed converter was tested in simulation in various operating conditions.**

Index Terms—**MPPT control, Photovoltaic systems, DC/DC converters.**

I. Introduction

Solar power has increased the attention for its significant potential in solving future energy problems and the foreseen severe shortage of energy sources. Photovoltaic (PV) inverter systems can be either stand-alone or grid-connected system. Grid-connected systems are used to reduce utility power [1], whereas standalone ones provide the required power without the use of utility [2], [3]. Furthermore, standalone systems dispense with the grid, so they need batteries that store the energy to supply load when the solar-energy production is low.

Storage batteries need a deep cycle to discharge a significant amount of the stored energy. The commonest deep-cycle battery is nickel-cadmium through it costs more than does lead-acid battery. Valve-regulated lead-acid (VRLA) battery has been widely used in PV applications recently. It is low-cost, maintenance-free, and considered the most recyclable among batteries [4]. For long battery life, a charge controller preventing complete discharging and surplus charging is needed. Battery life reduces when the PV-produced energy is low. Therefore, the converter needs maximum power point tracker (MPPT) control.

The conflict between charger control and MPPT control is that the charger control needs constant current and voltage to charge battery, whereas MPPT control produces variable voltage and current, which depends on PV power (that in turn depends on weather conditions). MPPT extracts additional power from PV array under specific conditions. It represents optimal load to PV array, producing an opportune voltage to the load. The PV cell yields exponential curves of the current and the voltage where the maximum power occurs at the curve's mutual knee [5]. The applied MPPT uses a type of control and logic to look for the knee, which in turn, allows converter to extract maximum power from the PV array. The tracking method, perturb and observe (P&O) [6], provides a new reference signal for the controller and extracts maximum power from the PV array.

Unlike research in MPPT and battery charger, combined research in MPPT for battery charger is rarely reported. In MPPT for battery charger, one control signal controls only one system (either charger or MPPT) at any single time. When the converter uses one control signal, the voltage supplying the battery is either not constant (the absence of voltage control possibly damaging battery), or constant (hence MPP cannot be achieved).

One of the most important issues that must be taken into consideration of the PV converter applications is the flowing of input current. Some converters like buck or buck-boost converter have a switch in series with the PV source. This series switch can lose half of the power available from the PV array. The other important thing is the independency of control functions. Therefore, the use of two control switches for each function will definitely improve the desired output for each function. Buck converter as a battery charger for standalone system is proposed in [7] and [8]. One control switch is used for SEPIC converter to control both MPPT and the battery charger [9]. In [10], the author used buck-boost converter to charge the battery with MPPT.

This paper describes a novel charger with fewer batteries, achieving maximum exploitation of power, and longer battery lifetime. The next sections of this paper are organized as follows: Section II describes the analysis of the overall system, Section III presents the ćuk-buck converter, Section IV presents the implementation of the control system, and Section V shows the results while Section VI draws the conclusions.

II. Overall System Description

Fig. 1 is a block diagram of the ćuk-buck MPPT charger, shown with the inverter. The ćuk-buck converter was supplied from the PV array and the output was connected to the batteries. The batteries were connected to the boost converter to step up battery voltage from 48V to 240V as inverter input. The inverter side including the boost converter output signal is controlled using PID controller. Two control signals control the converter. One tracks the maximum power, while the other controls the battery charger. The main function of the DC-DC converter is to increase or decrease the level of the voltage fed to the inverter. In this work, however, voltage level increases and decreases according to the MPPT scheme. The charge controller, furthermore, changes the voltage level to 58V charging the batteries. The

Manuscript received October 20, 2012; revised December 24, 2012. This work was supported in part by the UMPEDAC research center under Grant PV071-2011A.

The authors are with the UMPEDAC research center, University of Malaya, Kuala Lumpur, Malaysia (e-mail: akhateb84@hotmail.com; nasrudin@um.edu.my; jeyraj@um.edu.my).

DOI: 10.7763/JOCET.2013.V1.17

MPPT control signal changes the duty cycle of the pulse-width modulated (PWM) signal, which tracks the reference signal.

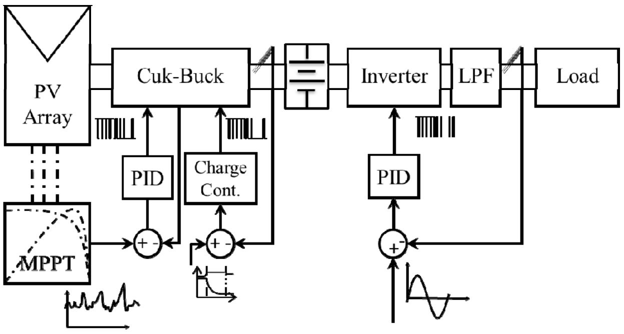

Fig. 1. Block diagram of the ćuk-buck and inverter-based PV system.

The reference signal of the MPPT output compared the DC voltage applied before the second switch. This signal is adaptive, its shape changes with weather conditions. The ćuk-buck's first switch, thus, feeds the second stage of the converter with the most suitable power. The second switch is fed by the control signal that compares the voltage and current applied on the battery following the three-stage control as illustrated in the fourth section. The circuit diagram of the ćuk-buck converter is shown in Fig. 2.

The controller operates the system in four operation states owing to the battery state of charge, the load, and the available power. The first state starts when the available PV power is less than the load power. The battery supplies the load automatically. The second state takes place when the available power is larger than the load power, and then, the undue power charges the battery. In the previous two states, the battery current supposedly cannot reach its reference current, but the signal generated by the battery current PID controller which is supplied with the most available power will generate zero-error signal.

The zero-error signal will charge the battery, and the maximum power operation will be already solved using the first switch controller which is MPPT-PID controller. In the third state, the available power of the PV modules is larger than the battery charging and the load power. In this case, the battery current will reach its reference current. As a result, the PV module will shift the reference voltage to a higher level than the MPPT voltage. Furthermore, the generated PV power will balance the load and the charging, as well. As a matter of fact, the third state cannot happen in the prescribed system because the PV array power is designed to be equal to the battery power and equal to the load power. In the fourth state, the battery voltage is lower than the level that can supply the load, and the available PV power is not sufficient to supply the load. In this case, a simple comparator switch is used to disconnect the load and reconnect if the battery voltage is larger than the lowest level of batteries.

III. Analysis of Ćuk-buck Converter

The ćuk-buck operation starts when the first switch S_1 turns on at time $t=0$, at which the moment current in inductor L_1 increases and the voltage on the capacitor turns off diode D_1. The first capacitor C_1 discharges its energy to the circuit when S_1 turns of at time $t=t_x$. The second switch S_2 instantaneously turns on depending on the feedback signal from the battery at time $t=t_y$. The current of S_2 passes through L_3, C_2, and the load. Once S_2 turns off at time $t=t_z$, the diode D_2 is connected owing to the energy stored in L_3. Fig. 2 shows the diodes and the switches, D_1, D_2, S_1, and S_2 providing synchronous switching action.

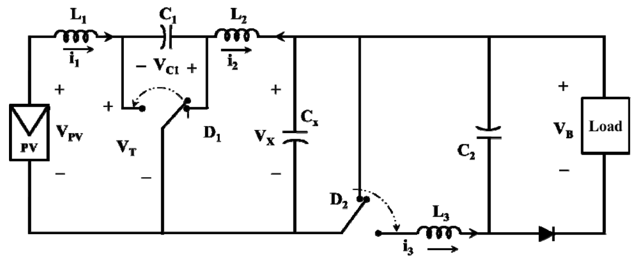

Fig. 2. Ćuk-buck circuit showing the synchronization of switches and diodes.

Now, a very small scope of the current through L_1 is taken as shown in Fig. 3, where the current I_1 can be shown linearly during time t_{on}. According to Fig. 3, equation (1) can be concluded.

$$V_{PV} = L_1 \frac{I_{tx} - I_{t0}}{t_{on}} = L_1 \frac{\Delta I_1}{t_{on}} \tag{1}$$

$$t_{on} = \frac{\Delta I_1 L_1}{V_{PV}} \tag{2}$$

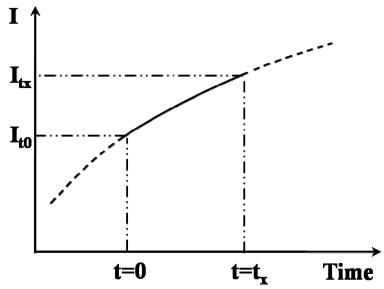

Fig. 3. Scope of very small current signal passing through inductor L_1.

During the charging of C_1, L_1 current falls linearly.

$$V_{PV} - V_{c1} = -L_1 \frac{\Delta I_1}{t_{off}} \tag{3}$$

$$t_{off} = -\frac{\Delta I_1 L_1}{V_{PV} - V_{c1}} \tag{4}$$

Expressing that the duty cycle of S_1 is D and the period is T, then:

$$t_{on} = DT \tag{5}$$

and,

$$t_{off} = (1-D)T \tag{6}$$

Substituting (5) and (6) in (4) and (2) respectively,

$$V_{c1} = \frac{V_{PV}}{1-D} \tag{7}$$

Assuming that the current of L_2 rises linearly from I_{tY} to I_{tZ} in time t_{on}, then:

$$V_{c1} + V_x = L_2 \frac{I_{tZ} - I_{tY}}{t_{on}} = \frac{L_2 \Delta I_2}{t_{on}} \tag{8}$$

Similarly,

$$t_{on} = \frac{L_2 \Delta I_2}{V_x + V_{c1}} \tag{9}$$

Moreover, at a small scope, the current falls linearly from I_{tZ} to I_{tY} in time t_{off}, so:

$$V_x = -L_2 \frac{\Delta I_2}{t_{off}} \tag{10}$$

where,

$$\Delta I_2 = I_{tZ} - I_{tY} \tag{11}$$

and,

$$t_{off} = \frac{-L_2 \Delta I_2}{V_x} \tag{12}$$

From (8) and (10),

$$\Delta I_2 = \frac{t_{on}\left(V_{c1} + V_x\right)}{L_2} = \frac{-t_{off} V_x}{L_2} \tag{13}$$

Then,

$$V_{c1} = -\frac{-V_x}{D} \tag{14}$$

From (7) and (14),

$$\frac{V_x}{V_{PV}} = \frac{-D}{1-D} \tag{15}$$

Assume that current in L_3 rises linearly,

$$V_B - V_x = L_3 \frac{\Delta I_3}{t_{on}} \tag{16}$$

and,

$$V_B = L_3 \frac{\Delta I_3}{t_{off}} \tag{17}$$

From (16) and (17), the following relation can be derived,

$$-t_{on} \frac{V_x + V_B}{L_3} + t_{off} \frac{V_B}{L_3} = 0 \tag{18}$$

Suppose that duty cycle of the second switch S_2 is δ, then:

$$t_{on} = \delta T \tag{19}$$

and

$$t_{off} = (1-\delta)T \tag{20}$$

Substituting (19) and (20) in (18), we can get,

$$(-V_x + V_B)\delta T + V_B(1-\delta)T = 0 \tag{21}$$

and,

$$-V_B + \delta V_x = 0 \tag{22}$$

Similarly,

$$\frac{V_B}{V_x} = \delta \qquad (23)$$

From (15) and (23),

$$\frac{V_B}{V_{PV}} = -\frac{\delta D}{1-D} \qquad (23)$$

where δ is the duty cycle that controls the battery charger and D is the duty cycle that controls the maximum-power-point tracker.

The time diagram of voltages and currents shown in Fig. 2 is presented in Fig. 4, where the values of inductors and capacitors are properly chosen for very low output voltage ripples. The voltage and current waveforms are working in continuous conduction mode. Owing to the parameters, the instantaneous inductors current does not fall to zero at any time during the switching cycle.

IV. Control for Ćuk-buck Converter

Three stages are presented for the charger. The first stage is the constant current reference signal with 0.175C that was used to charge the battery 85%. The second stage is the constant voltage control, which applied 58V to the battery till it was fully charged. The last stage is the floating charge, which applied a constant 54V to the battery, and the charge current was below 0.05C. The use of the floating charge extends the battery life time. Thus, the battery charge current was large in the first stage, then it was gradually reduced in the next stage [11].

The reference signals for both the voltage and the current are compared with the feedback signals. A triangular carrier signal was also compared with the error signals and generated the PWM that fed the second switch of the ćuk-buck converter.

The MPPT control technique is applied to achieve a new reference voltage for the PID controller. It changes the duty ratio of the PWM signal for the first switch of the ćuk-buck converter. The P&O algorithm has a simple structure and requires only a few parameters (i.e. power and voltage), so it is extensively used in many MPPT systems [12]-[16]. Furthermore, it can be easily applied to any PV panel, regardless of the PV module's characteristics for the MPPT process.

The P&O method periodically perturbs duty ratio (through reference signal) and compares instantaneous power with past power (before perturbation). Based on this comparison, the PV voltage determines the direction of the next perturbation. Fig. 5 shows the flowchart of the P&O method. It simply shows that if the power slope and the voltage slope increase, the reference voltage will increase; otherwise, it will decrease.

Step-size of the P&O method affects two parameters: accuracy and speed. Accuracy increases when step-size decreases but when environmental conditions change rapidly it causes slow response. Larger step-size means faster but less accurate MPPT operation and larger intrinsic oscillations around the maximum power point in steady state. Therefore, for high speed and accuracy, step-size should be chosen appropriately as it shouldn't be very small or big. It should fit with the weather changes.

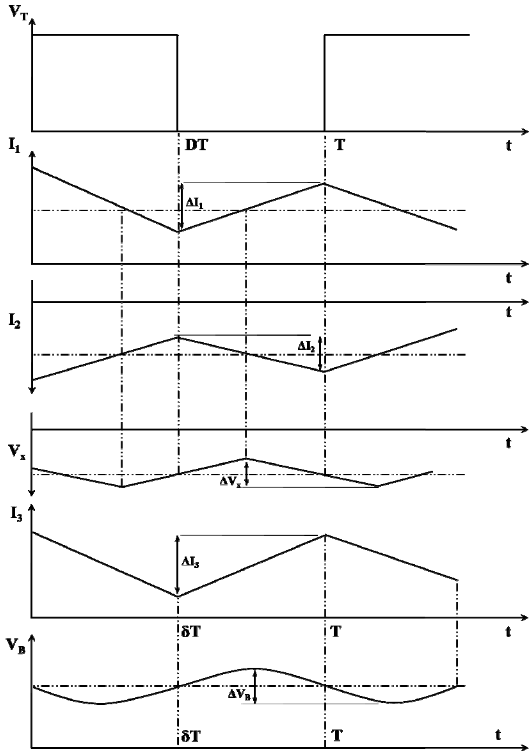

Fig. 4. Time diagram of voltage and current waveforms of ćuk-buck converter

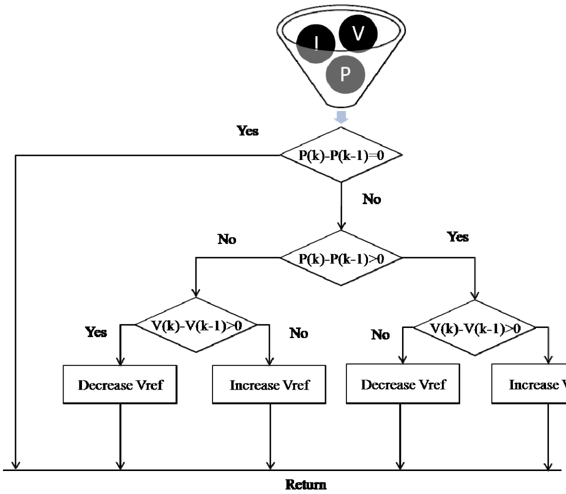

Fig. 5. Flowchart of P&O based MPPT method.

The duty ratio $\delta_{(k)}$ of the PWM is adjusted either by adding or subtracting the previous duty ratio $\delta_{(k-1)}$ with the duty ratio perturbation step-size $\Delta\delta$ as shown in (25).

$$\delta_{(k)} = \delta_{(k-1)} \pm \Delta\delta \tag{25}$$

Fig. 6 shows the curves of power vs. voltage, at 25°*C* and 50°*C*, for radiation ranging from 250*W/m*^{2} to 1000*W/m*^{2}. The simulation values for the PV modules and the number of the PV arrays duplicated those of the experiment setup.

The reference voltage signal tracking the maximum power is illustrated in Fig. 7. The relation between Figs. 8 and 9 can now be determined easily. The maximum power occurred around 120*V* to 135*V* owing to radiation variations.

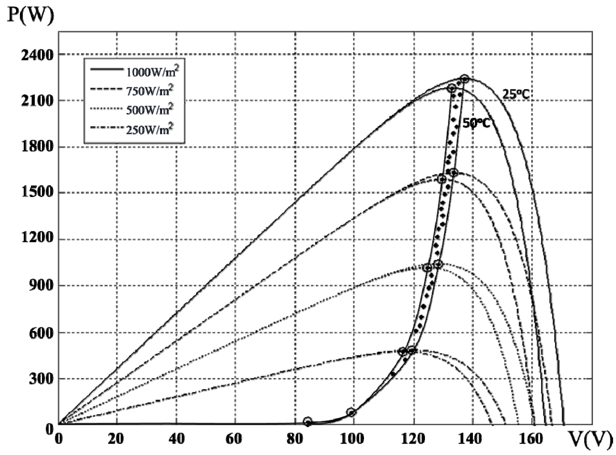

Fig. 6. Power-Voltage (P-V) curves for the prescribed PV array.

V. Simulation Results

A simulation on MATLAB-Simulink verified the practical implementation of the proposed converter. Fig. 7 presents the reference signal for the output of the ćuk part; it tracked the maximum power. Fig. 8 shows the voltage and current output signals of the ćuk part of the MPPT-based converter. The signals were noticeably not smooth; they carried a component of the maximum power between voltage and current. The voltage signal (Fig. 8) is similar to the reference signal (Fig. 7), while the error signal approached zero (see Fig. 9).

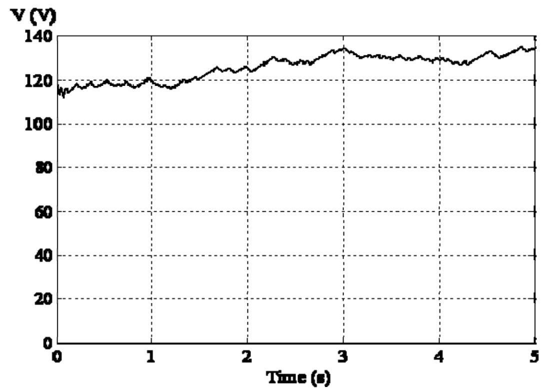

Fig. 7. Reference voltage, V_{REF}, tracking maximum power.

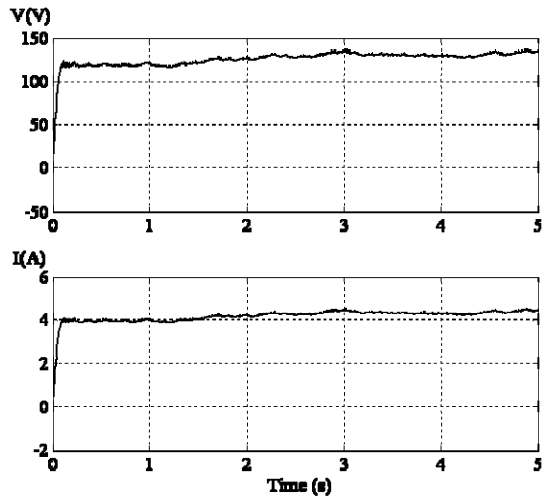

Fig. 8. The ćuk-buck converter's output voltage and current of the MPPT part.

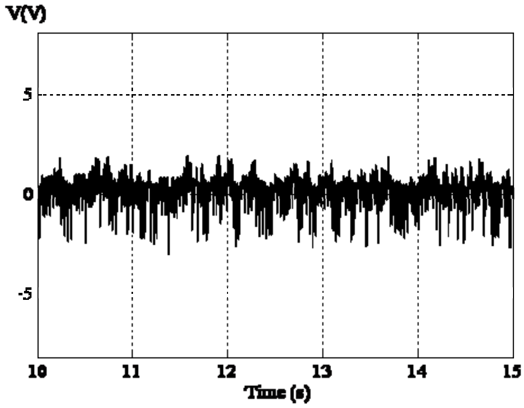

Fig. 9. Voltage error signal (ΔV) corresponding to Fig. 8.

Fig. 10 presents the charging voltage, the current, and the state of charge (SOC). The constant current control charges the battery to 85% charged state within 4.52 hours. Then, constant voltage charging fills the battery within 0.89 hours. After that, floating charging is applied to keep the battery charged. Fig. 11 shows the discharge characteristics; the battery was discharged within 5 hours at a constant 3.5kW load with discharging time increasing for lower-value loads (12.5 hours for a constant 1.4kW load and 24 hour for a constant 720W load).

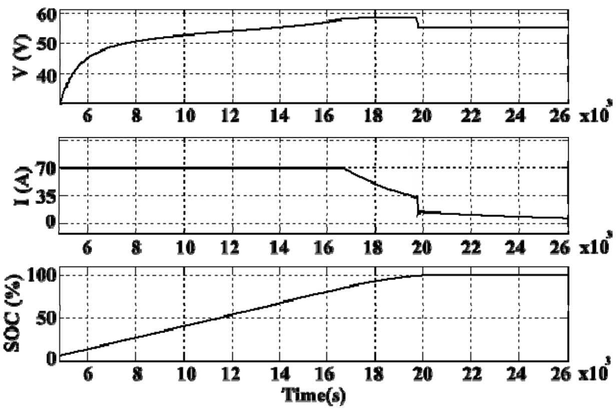

Fig. 10. Charging voltage, current, and state of charge (SOC).

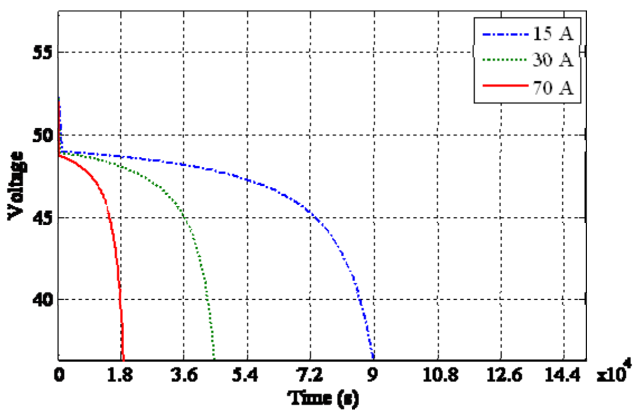

Fig. 11. Discharge characteristics of series four 100Ah 12V batteries.

References

[1] M. Gómez-González and F. Jurado, "A binary shuffled frog-leaping algorithm for the optimal placement and sizing of photovoltaics grid-connected systems," *International Review of Electrical Engineering (IREE),* vol. 6, no. 1, pp. 452-458, February 2011.

[2] L. Padmavathi and P. Janakiraman, "Self-tuned feed-forward compensation for harmonic reduction in single-phase low-voltage inverters," *IEEE Transactions on Industrial Electronics,* vol. 58, no. 10, pp. 4753-4762, October 2011.

[3] B. Mirafzal, M. Saghaleini, and A. Kaviani, "An SVPWM-based switching pattern for stand-alone and grid-connected three-phase single-stage boost inverters," *IEEE Transactions on Power Electronics,* vol. 26, no. 4, pp. 1102-1111, April 2011.

[4] H. Fakham, D. Lu, and B. Francois, "Power control design of a battery charger in a hybrid active PV generator for load-following applications," *IEEE Transactions on Industrial Electronics,* vol. 58, no. 1, pp. 85-94, June 2011.

[5] Y. Ji, D. Jung, J. Kim, J. Kim, T. Lee, and C. Won, "A real maximum Power Point Tracking Method for Mismatching Compensation in PV array under partially shaded conditions," *IEEE Transactions on Industrial Electronics,* vol. 26, no. 4, pp. 1001-1009, April 2011.

[6] A. K. Abdelsalam, A. M. Massoud, S. Ahmed, and P. N. Enjeti, "High-performance adaptive perturb and observe MPPT technique for photovoltaic-based microgrids," *IEEE Transactions on Industrial Electronics,* vol. 26, no. 4, pp. 1010-1021, April 2011.

[7] K. Lo, Y. Chen, and Y. Chang, "MPPT Battery Charger for Stand-Alone Wind Power System," *IEEE Transactions on Industrial Electronics,* vol. 26, no. 6, pp. 1631-1638, June 2011.

[8] E. Koutroulis and K. Kalaitzakis, "Novel battery charging regulation system for photovoltaic applications," *IEE Proceedings-Electric Power Applications,* vol. 151, no. 2, pp. 191-197, March 2004.

[9] S. J. Chiang, H. Shieh, and M. Chen, "Modeling and control of PV charger system with SEPIC converter," *IEEE Transactions on Industrial Electronics,* vol. 56, no. 11, pp. 4344-4343, November 2009.

[10] V. Scarpa, S. Buso, and G. Spiazzi, "Low-complexity MPPT technique exploiting the PV module MPP locus characterization," *IEEE Transactions on Industrial Electronics,* vol. 56, no. 5, pp. 1531-1538, May 2009.

[11] B. Chen and Y. Lai, "New digital-controlled technique for battery charger with constant current and voltage control without current feedback," *IEEE Transactions on Industrial Electronics,* vol. 59, no. 3, pp. 1545-1553, March 2012.

[12] A. El Khateb, N. A. Rahim, and J. Selvaraj, "Optimized PID controller for both single phase inverter and MPPT SEPIC DC/DC converter of PV module," *IEEE International Electric Machines & Drives Conference (IEMDC)*, pp. 1036-1041, June 2011.

[13] Subiyanto, A. Mohamed, and M. A. Hannan, "Photovoltaic maximum power point tracking controller using a new high performance boost converter," *International Review of Electrical Engineering (IREE),* vol. 5, no. 6, pp. 2535-2545, December 2010.

[14] N. A. Rahim and J. Selvaraj, "Multistring five-level inverter with novel PWM control scheme for PV application," *IEEE Transactions on Industrial Electronics,* vol. 57, no. 6, pp. 2111-2123, June 2010.

[15] S. L. Brunton, C. W. Rowley, S. R. Kulkarni, and C. Clarkson, "Maximum power point tracking for photovoltaic optimization using ripple-based extremum seeking control," *IEEE Transactions on Power Electronics,* vol. 25, no. 10, pp. 2531-2540, October 2010.

[16] J. Selvaraj and N. A. Rahim, "Multilevel inverter for grid-connected PV systems employing digital PI controller," *IEEE Transactions on Industrial electronics,* vol. 56, no. 1, pp. 149-158, January 2009.

Ahmad H. El Khateb received the B.Sc. and M.Sc. degrees in Electrical Engineering from the Islamic University of Gaza, Palestine, in 2005 and 2007 respectively. He is currently working toward Ph.D. degree in Electrical Engineering and joining UMPEDAC as Research Engineer.

He has been enrolled in Electrical Engineering Department at the Islamic University of Gaza as a teaching assistant from 2005 to 2007 and lecturer from 2007 to 2010. His main research interests are control systems, power electronics, fuzzy logic control, and renewable energy.

Nasrudin A. Rahim was born in Johor, Malaysia, in 1960. He received the B.Sc. (Hons.) and M.Sc. degrees from the University of Strathclyde, Glasgow, U.K., and the Ph.D. degree from Heriot–Watt University, Edinburgh, U.K., in 1995. He is currently a Professor with the Department of Electrical Engineering, University of Malaya, Kuala Lumpur, Malaysia, where he is also the Director of UMPEDAC research center and Chairman of University of Malaya Advanced Engineering & Technology Research Cluster.

He has 17 years of teaching experience and has authored and coauthored more than 300 papers.

Prof. Rahim is a Fellow of the Institution of Engineering and Technology, UK, and a Chartered Engineer. He had been Chairman of

IEEE Power Engineering Society/Electric Machinery Committee Motor Subcommittee Working Group 8 (WG-8) covering reluctance motors. His research interests include power electronics, real-time control systems, electrical drives, and renewable energy.

Jeyraj Selvaraj received the B.Eng. (Hons.) degree from Multimedia University, Cyberjaya, Malaysia, in 2002, the M.Sc. degree in power electronics and drives jointly from the University of Birmingham, Birmingham, U.K., and the University of Nottingham, Nottingham, U.K., in 2004, and the Ph.D. degree from the University of Malaya, Kuala Lumpur, Malaysia, in 2009.

He is currently with UMPEDAC research center, Faculty of Engineering, University of Malaya.

Dr. Selvaraj research interests are single and three-phase multilevel inverters, digital PI current-control techniques, photovoltaic inverters, and dc–dc converters.